Supplementary Information

DNA-controlled aggregation of virus like particles – mimicking a tetherin-like mechanism

Daniela Serien, Christiane Grimm, Jürgen Liebscher, Andreas Herrmann, and Anna Arbuzova

Milli-Q water and UV-clean (Uvasol) chloroform were used. 100 mM KCl (Sigma, USA), 10 mM HEPES (Roth, Karlsruhe, Germany) buffer was adjusted to pH 7.4 with KOH. The buffer was filtered by a sterile 220 nm PES syringe filter (Roth, Karlsruhe, Germany) and degased at 30 °C for 30 minutes. 1-Palmitoyl-2-oleoyl-sn-glycero-3-phosphocholine (POPC) and 1, 2-dipalmitoyl-sn-glycero-3-phosphoethanolamine-N-(7-nitro-2-1,3-benzoxadiazol-4-yl) (N-NBD- DPPE) were purchased from Avanti Polar Lipids Inc. (Alabaster, Alabama, USA). Oligonucleotides $(dT)_{20}$, $(dA)_{20}$, tetramethylrhodamine (TMR)-XR6160 labeled 3´Rh$(dT)_{20}$, and 3´Rh$(dA)_{20}$, and α-tocopherol modified TL$(dT)_{18}$L$(dT)_5$, LiNA, were synthesized by BioTez (Berlin, Germany), while α-tocopherol desoxycytidine phosphoamidide, L

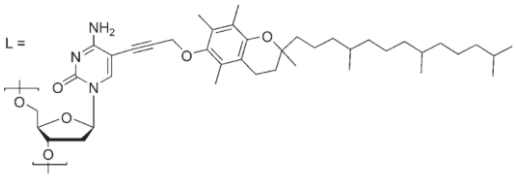

,

was synthesized as described elsewhere.[1,2]

POPC or 1.5 mol% *N*-NBD-DPPE/ 98.5 mol% POPC in chloroform were added to a 50 mL round-bottomed flask and dried on a rotary evaporator to obtain a thin lipid film, rehydrated with buffer immediately afterwards. Five freeze-thaw cycles were performed. Lipid suspension was extruded 10 times using an extruder (Lipex Biomembranes Inc., Vancouver, Canada) with a 100 nm filter (Whatman) at 40 °C.

90° light scattering time traces were measured with slit width 1 nm using a spectrofluorometer (Fluoromax-4, Horiba Jobin Yvon GmbH), or a luminescence spectrometer (Aminco-Bowman-Series 2, Thermo Spectronic). An electronic thermometer was inserted into the samples. Heating and cooling of the sample was linear. Temperature was varied in the range from 20 to 52 °C.

The lipid to LiNA ratio was 2000:1, when not stated otherwise. Kinetics of lipid vesicle aggregation was investigated at λ = 400 nm, 20 °C, and DNA hybridization at 270 nm using UV-Vis scanning spectrophotometer (Shimadzu), 5 nm slits. Microscopy images were obtained on an Olympus IX-81 (Olympus, Hamburg, Germany) with a cooled CCD camera (SPOT Slider, Visitron Systems, Puchheim, Germany) using a 63× or 100× oil immersion objective. Rhodamine signals were measured for 10 ms with fluorescence filter sets BA590, BP530-550 and DM570, NBD signals for 100 ms with BA510-550, BP470-490 and DM505, respectively. mCherry signals were measured for 100 ms with fluorescence filter sets BA590, BP530-550 and DM570.

Usually 200 nM of an oligonucleotide were used. All measurements were performed in quartz cuvettes with permanent magnetic stirring. Time traces were obtained using 1 mL sample volume with 1s increment and integration time.

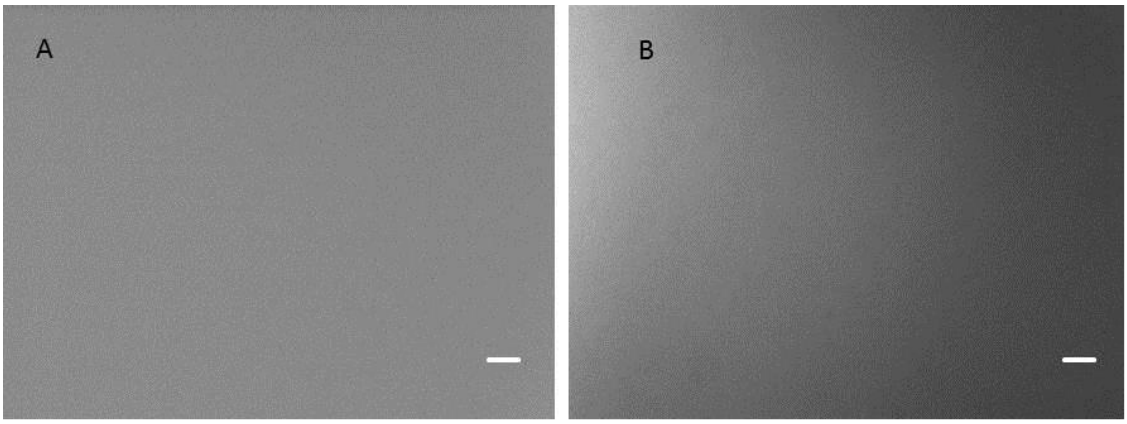

Figure S1. Rhodamine fluorescence images of A) a sample containing 3´Rh$(dA)_{20}$, 200 nM, and POPC/NBD-PE vesicles, 400 µM, without the LiNA, B) a sample containing non-complementary strand, 3´Rh$(dT)_{20}$, the LiNA, 200 nM each, and POPC/NBD-PE vesicles, 400 µM. Scale bars correspond to 10 µm.

Disaggregation/aggregation was reversible and reproducible on the very same sample as well as on different samples (not shown). Note, light scattering intensities of POPC vesicles alone decreased with increasing temperature, and therefore a control trace of the changes for a sample containing POPC vesicles only (the same concentration) was linearly subtracted from the data shown in Figure 2B.

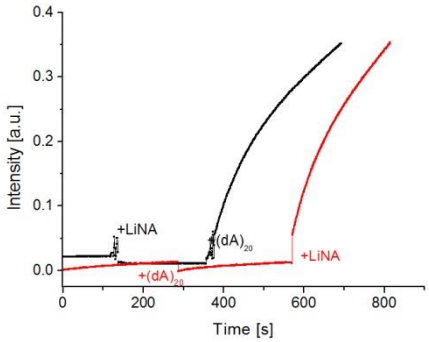

Figure S2. Sequence of the oligonucleotide addition was not essential.

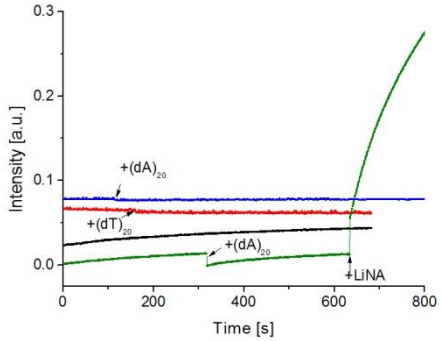

Figure S3. Only in presence of both the lipophilic oligonucleotide, the LiNA, and the complementary DNA strand, $(dA)_{20}$ 200 nM each, POPC vesicle aggregated (700 µM lipid, green). No aggregation of POPC vesicles (700 µM) when only the complementary strand (blue), LiNA (black), or LiNA and non-complementary strand $(dT)_{20}$ (red) at 20 °C were added at 200 nM each.

Liposomes did not fuse as no recovery of *N*-NBD-DPPE fluorescence after photobleaching was observed, in agreement with previously demonstrated assembly of intact liposomes by LiNAs of similar length (not shown).[3,4]

Collision-diffusion mechanism of aggregation

The differential equation for collision-diffusion based bimolecular reaction of two equal particles is

$$r = kc^2$$

where r is the reaction rate, k is the rate constant and *c* is the concentration of the particle. Due to the proportionality, vesicle concentration ratio corresponds to lipid concentration ratio $R=c/c_0$, where c_0= 55 μM here.

$$r(R)= kc_0^2 R^2$$

A polynomial function $f(x) = a_0 + a_1 x^{b_1}$ was fitted to the data. For the vesicle concentration of 0 μM no aggregation occurs, hence, $a_0 = 0\ s^{-1}$ was assumed.

Initial aggregation rate r was obtained as a slope of the best linear fit to data, at least 20 data points, starting at the time point of the complementary strand addition, $R^2 > 0.9$ and chosen by lowest χ^2. We found that the initial rate of the lipid vesicle aggregation had second-order with respect to vesicle concentration. The simplest explanation is that, in agreement with the above described bimolecular reaction kinetics mechanism; vesicle aggregation is limited by vesicle-vesicle collision. However, calcium- induced aggregation and fusion of small phosphatidylserine vesicles was reported to have an apparent second-order kinetics[5] and the initial rate of dipalmitoylphosphatidylcholine vesicle fusion below the phase transition temperature was also shown to be approximately second order regarding vesicle concentration, although simple vesicle-vesicle collision was presumably not the rate limiting step.[6]

Virus like particles

Lacking regulatory proteins and genetic material, VLPs are used in many studies as they, although resembling morphologically and antigenically native virions, are not infectious.[7] Assembly, budding, and release of VLPs in human embryonic kidney 293T (HEK-293T) cells requires at least expression of Gag and the N-terminal domain of the capsid protein.[8,9] Co-expression of Gag, capsid, and spike proteins led to the formation and release of VLPs bearing the spike glycoproteins on the VLP surface. VLPs were purified by ultracentrifugation through a sucrose gradient to a purity of greater than 80%. Obtained 100–120 nm VLPs included approximately 1500–1800 Gag monomers.[10]

1. Kurz, A. *et al.* Lipid-anchored oligonucleotides for stable double-helix formation in distinct membrane domains. *Angew. Chem. Int. Ed. Engl.* **45,** 4440–4444 (2006).

2. Flasche, W., Cismas, C., Herrmann, A. & Liebscher, J. Lipophilic Nucleosides by Sonogashira Coupling. *Synthesis (Stuttg).* **2004,** 2335–2341 (2004).

3. Loew, M. *et al.* Controlled assembly of vesicle-based nanocontainers on layer-by-layer particles via DNA hybridization. *Small* **5,** 320–323 (2009).

4. Dave, N. & Liu, J. Programmable assembly of DNA-functionalized liposomes by DNA. *ACS Nano* **5,** 1304–1312 (2011).

5. Wilschut, J., Duzgunes, N., Fraley, R. & Papahadjopoulos, D. Studies on the mechanism of membrane fusion: kinetics of calcium ion induced fusion of phosphatidylserine vesicles

followed by a new assay for mixing of aqueous vesicle contents. *Biochemistry* **19,** 6011–6021 (1980).

6. Wong, M., Anthony, F. H., Tillack, T. W. & Thompson, T. E. Fusion of dipalmitoylphosphatidylcholine vesicles at 4 degrees C. *Biochemistry* **21,** 4126–4132 (1982).

7. Deml, L., Speth, C., Dierich, M. P., Wolf, H. & Wagner, R. Recombinant HIV-1 Pr55gag virus-like particles: potent stimulators of innate and acquired immune responses. *Mol. Immunol.* **42,** 259–277 (2005).

8. Jalaguier, P., Turcotte, K., Danylo, A., Cantin, R. & Tremblay, M. J. Efficient production of HIV-1 virus-like particles from a mammalian expression vector requires the N-terminal capsid domain. *PLoS One* **6,** e28314 (2011).

9. Huang, M., Orenstein, J. M., Martin, M. A. & Freed, E. O. p6Gag is required for particle production from full-length human immunodeficiency virus type 1 molecular clones expressing protease. *J. Virol.* **69,** 6810–6818 (1995).

10. Briggs, J. a G. & Kräusslich, H.-G. The molecular architecture of HIV. *J. Mol. Biol.* **410,** 491–500 (2011).